Tracer Studies of High-Shear Granulation: I. Experimental Results

J. M. K. Pearson
Dept. of Chemical Engineering, The University of Cambridge, Cambridge, U.K.

M. J. Hounslow
Particle Products Group, Dept. of Chemical and Process Engineering, The University of Sheffield, Sheffield, U.K.

T. Instone
Unilever Research, Port Sunlight Laboratory, U.K.

Previous work has shown that attempts to determine the rates of processes active during granulation inevitably confound the effects of granule age and size; since as an experiment progresses, both the age and size of granules increases. In the current work, tracer experiments have been developed, and verified, to unconfound those effects. Qualitative analysis of the tracer data shows that granule breakage is occurring at a significant rate and that the breakage, or selection rate, appears to depend on granule age, but not on granule size.

Introduction

Granulation techniques are used in the manufacture of a multitude of chemical products and although, for many of these products, the optimal range of, for example, size and porosity, are known, manufacturing within these bounds is difficult. This work focuses on just such a process: high-shear granulation. Although this process has been used for some time, it is not well understood. Particular problems are those of scale-up and mixer design, and the effects of various process variables on the rate of granulation and on granule properties. The work presented here aims at making an initial step towards quantifying the kinetics of granulation so that a detailed quantitative analysis of the effects of some of these other parameters may be made later.

In a previous article (Pearson et al., 1998), it was demonstrated that with the most standard of kinetic analyses, there is a confounding between the effects of granule age and size on the rate at which granulation occurs. We also mentioned that the use of tracers might be a suitable tool with which to gain a greater understanding of this problem. In this article, the use of tracers is described more fully and the results are examined with specific reference to their implications for breakage.

The work presented here is, in some ways, similar to that of Ramaker et al. (1997). In both cases, high-shear granulation is studied, and tracers are added; the principal difference is in the method of tracer preparation. Ramaker et al. used a higher impeller speed to manufacture smaller granules for use as tracers, whereas, we have sieved out different fractions of granules made using the same impeller speed as standard granules to obtain the desired tracer size. In this way, as will be shown, we may be confident that the tracers behave in the same way as other granules. Further differences also appear in the way that the data are analyzed.

Experimental Techniques

The experiments reported here were carried out using two high-shear mixers. Principally, the Fukae FS30, used by Knight (1993), was used. This is a 30 L pilot-scale mixer with a base-mounted impeller and a side-mounted chopper. The impeller can be operated at speeds up to 300 rpm, and the chopper has a maximum speed of 3,000 rpm. The mixer is jacketed and is supplied with cold water and steam, the relative flow rates of which can be adjusted in order to obtain the desired operating temperature in the vessel.

The second mixer was the Zanchetta RotoJunior used by Scott et al. (2000). This is a 10-L laboratory-scale mixer. Again, it has a base-mounted impeller that can be operated at speeds up to 850 rpm. The chopper in this mixer is mounted in the lid and has a maximum speed of 1,400 rpm. This mixer is also jacketed to allow for product temperature control. The

---

Correspondence concerning this article should be addressed to M. J. Hounslow.

smaller mixer was used to carry out the experiments on the validation of tracer granules. All other experiments were carried out in the larger mixer.

The powder used in these experiments was *Durcal* 15, a brand of milled calcium carbonate supplied by Croxton and Garry, Dorking, Surrey, U.K. This has a measured mean size of 13 μm. Flake polyethylene glycol (PEG) 1,500 was used as the binder. This has an average molecular weight of 1,500 Daltons and melts at around 45°C. The operating temperature of 55°C ensures that the binder is present as a liquid.

Standard granules were manufactured in the FS30 using the following protocol:

- The flow rates of the steam and water were set in order to obtain the desired jacket temperature.
- *Durcal* (20 kg) was weighed into the mixer.
- The mixer was operated with the impeller at 300 rpm and the chopper at 3,000 rpm will until the powder reached the operating temperature.
- The mixer was stopped, and 2.8 kg of solid PEG were added.
- The mixer was restarted with the impeller at 150 rpm and the chopper still at 3,000 rpm.
- At intervals over the next 20 min, samples were taken.

Sampling was carried out using the method of Knight et al. (1998).

In order to make tracer granules, essentially the same procedure was followed. Blue dye, Patent V80, was added to the *Durcal* in a powdered form prior to preheating. In 20 kg of powder, 600 g of dye was used. The experiment was continued according to the protocol for the standard granules. No interim samples were taken, but once the required tracer age was achieved, the mixer was stopped, and its entire contents were removed and cooled. This mass of granules was then sieved into the required size fractions and retained for future use.

Experiments in which preformed tracer granules were added to a standard experiment were carried out as follows:

- The preformed tracer granules were placed in a metal container in an oven set at 60°C at least 1 h before they were required, in order to be heated to the operating temperature.
- A granulation experiment was carried out following the standard protocol with the preheating and binder addition stages; samples were taken after 4 and 8 min.
- Prior to restarting the mixer after the removal of the 8 min sample, the preheated tracer was poured into the bowl, and the mixer was then restarted.
- The experiment was continued in the usual way with samples withdrawn and cooled for later analysis.

Tracer granules were added 8 min into the standard experiment irrespective of their ages. This allowed for study of the effects of granule age on the process kinetics.

Material was assayed for dye content in the following fashion. A known mass of granules of a given size was dissolved in a known mass of distilled water; the resulting suspension was then vacuum-filtered through a 1 μm filter membrane in order to obtain a solids-free solution. Since the dye is soluble in water, it remained in the filtrate, giving it a blue color—subsequently measured by spectrophotometry.

In order to calibrate the spectrophotometer, solutions were made using spare tracer granules that had not been used in an experiment. These granules have the advantage of containing a known mass of dye. Therefore, if different quantities of water were used in the dissolution stage, then different concentrations of dye were obtained. These related to different degrees of light absorption at the correct wavelength. The values of adsorption were plotted against concentration, and a linear fit was made to the points. The equation of the fitted line was then used to back-calculate the dye concentration in the experimental samples.

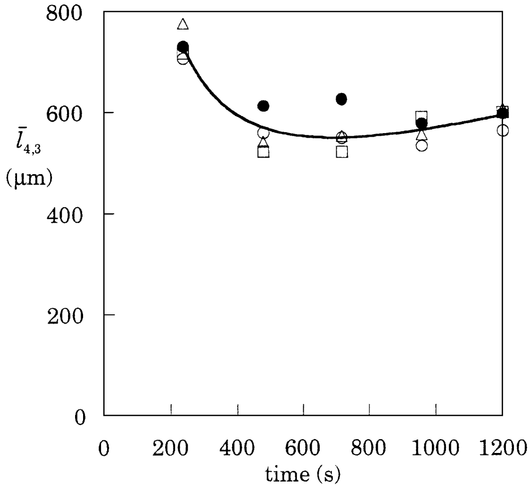

Figure 1. Four-three mean size as a function of time.

Open symbols are from standard experiments; closed from one with dye added.

The wavelength at which all of the samples were scanned was chosen by carrying out a broad-spectrum scan of one of the calibration samples. One major peak and one minor peak would appear on these, and the wavelength at which the major peak appeared was chosen for scanning. Typically, this peak was between 635 and 640 nm.

Tracer validation

For the data obtained from the tracer experiments to be useful, it is necessary that the tracer granules be representative of the standard granules that they are mimicking. Therefore, three properties of the tracer granules were compared with the standard granules in order to ascertain the effectiveness of the tracer granules.

Three standard experiments, and one to which dye had been added (as though to manufacture tracer granules), were carried out in the RotoJunior mixer for the purpose of comparing the granulation rates obtained. Initially, the means granule sizes were compared. In Figure 1, the closed symbols represent the results from the dye containing experiment, designated CM98/004, and the open symbols represent the results of three standard experiments, designated CM98/001–CM98/003.

Clearly, the results displayed in Figure 1 show good agreement with one another, suggesting that the dye containing granules might behave in the same way as the standard granules. However, it should be noted that simply comparing values of the mean granule size is not necessarily a good way of following a granulation process, and, therefore, the normalized mass density functions are also considered. These are

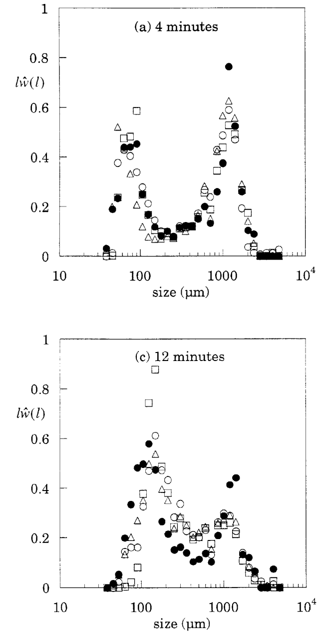

Figure 2. Comparison of size distributions produced in standard and dyed experiments.

Symbols have the meaning given in Figure 1.

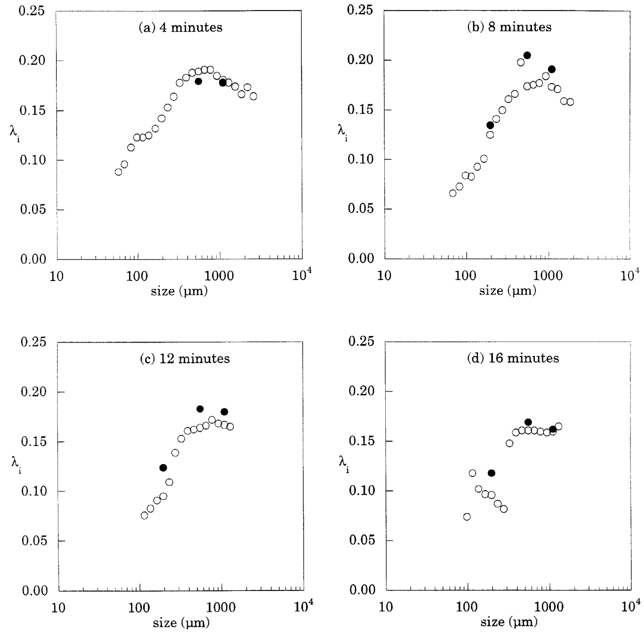

Figure 3. Ratio of liquid-to-solid found in granules as a function of size.

Open symbols are from a standard experiment; closed symbols are from one with dye added.

plotted in Figure 2. Although there is some variation in these results, the graphs in Figure 2 show that the particle-size distributions of the dye-containing granules are comparable to those of the standard granules. Certainly, within the degree of scatter of the standard experiments, these tracer granules are seen to behave in the same way as their standard counterparts.

In addition, the thermogravimetric technique of Knight et al. (1998) was used to determine the liquid-to-solid ratio of granules as a function of their age and size. The results of these experiments are shown in Figure 3. Again, the closed symbols represent the dye-containing granules, and the open symbols represent the results of the standard experiments. These results show that this particular internal characteristic of the standard granules is also well represented by the tracer granules. Overall, the experiments discussed in this section have shown that the behavior of tracer-granules does not differ significantly from that of standard granules.

Theory

Figure 4 shows a typical calibration curve for the spectrophotometry carried out during this work. Clearly, this is a linear plot, and so a straight line is fitted to the data. The equation of this line takes the following form

$$A_b = \mu x + \nu \tag{1}$$

where A_b is the absorption, x is the dye mass fraction in the sample, and μ and ν are the calibration constants. When the granules are dissolved, there is a certain mass of dye contained within a suspension of water, PEG, *Durcal*, and dye. Although the *Durcal* is filtered out to leave a clear solution, the concentration of dye does not change, and so the dye mass fraction continues to be measured on this basis. Thus, the dye mass fraction in a given size interval is given by

$$x_i = \frac{A_{bi} - \nu}{\mu} \tag{2}$$

where the subscript i refers to a specific value in size fraction i. The mass of granules retained on a sieve is w_i, and the mass of granules used for filtration is g_i. The mass of distilled water used for dissolution of the PEG is h_i. In addition to these known quantities, the masses of *Durcal*, PEG, and

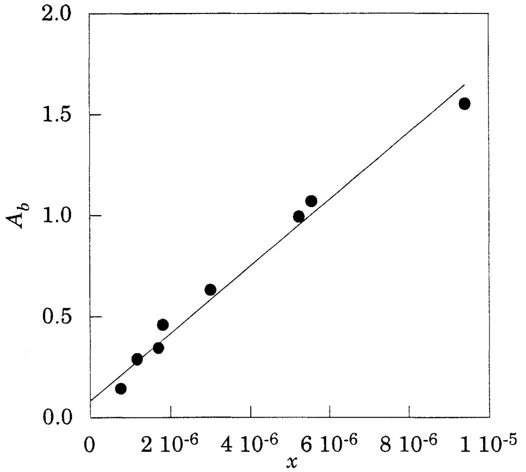

Figure 4. Typical calibration plot showing the absorption of a solution as a function of the mass fraction of dye therein.

dye within the granules used in the assay need to be defined. They are given the symbols s_i, p_i, and d_i, respectively. Given these quantities, the following statements can be made

$$x_i = \frac{d_i}{d_i + p_i + h_i} \tag{3}$$

$$p_i = \lambda s_i \tag{4}$$

$$\begin{aligned} g_i &= s_i + p_i + d_i \\ &= s_i(1+\lambda) + d_i \end{aligned} \tag{5}$$

where λ is the predefined liquid to solid ratio of the whole batch. From Eq. 3, we can say that

$$\begin{aligned} d_i &= x_i(d_i + p_i + h_i) \\ d_i(1 - x_i) &= x_i(p_i + h_i) \end{aligned} \tag{6}$$

Using Eq. 4, the following is obtained

$$d_i(1 - x_i) = x_i(h_i + \lambda s_i) \tag{7}$$

Now, from Eq. 5 we get

$$s_i = \frac{g_i - d_i}{1 + \lambda} \tag{8}$$

and substituting Eq. 8 into Eq. 7 gives

$$\begin{aligned} d_i(1 - x_i) &= x_i\left[h_i + \lambda\left(\frac{g_i - d_i}{1+\lambda}\right)\right] \\ d_i\left(1 - x_i + \frac{x_i\lambda}{1+\lambda}\right) &= x_i\left[h_i + \lambda\left(\frac{g_i}{1+\lambda}\right)\right] \\ d_i &= \frac{x_i\left[h_i + \lambda\left(\frac{g_i}{1+\lambda}\right)\right]}{\left(1 - \frac{x_i}{1+\lambda}\right)} \end{aligned} \tag{9}$$

Thus, we have obtained an expression for the mass of dye in the granules that were used to carry out the dye assay. However, this in itself is not a particularly useful quantity, and so further calculations are necessary.

First, the mass of dye in a sieve fraction is calculated, normalized to 1 kg of granules. This quantity is given the symbol ΔM_i, and is calculated thus

$$\Delta M_i = \frac{d_i}{g_i}\frac{w_i}{\Sigma w_i} \tag{10}$$

From this, the normalized dye, or tracer mass density (TMD) distribution $\hat{M}(\bar{l}_i)$, can be calculated

$$\hat{M}(\bar{l}_i) = \frac{\Delta M_i}{\Sigma \Delta M_i}\frac{1}{(l_{i+1} - l_i)} \tag{11}$$

In this final equation, l_i represents the lower bound on particle size in the ith size interval.

When tracers are added to a standard experiment, the nature of the method is such that all of the dye is contained within granules greater than a certain size. It was quickly noticed when these experiments were carried out that the dyed material was being transferred to other sizes of granules, both larger than, and smaller than, the tracer granules.

Dye can be transferred to smaller-size intervals by two mechanisms: breakage of granules and direct transfer of dye from larger granules to smaller ones, perhaps by "wicking" of the dye-containing binder when two granules collide, but do not adhere. As the results introduced later will show, in one case, in excess of 90% of the tracer mass is transferred to smaller sizes. For this to be accomplished by wicking would require a quite inconceivable mobility of the binder and dye. We conclude that transfer of dye to smaller size classes is by breakage.

The mass fraction of dye in a given size fraction can be calculated by dividing the mass of dye in an interval, as given by Eq. 10, by the sum of these masses. If dye that appears in sizes smaller than the initial tracer size is said to be "relegated," the fraction of dye relegated can be calculated by summing the dye mass fractions over all sizes smaller than the initial tracer size. This relegated dye mass fraction is given the symbol χ.

Normalized tracer mass distribution, with the quantity χ shown hatched, and the quantity $1 - \chi$ shown as solid color is shown in Figure 5. It can be seen that the rate at which dyed material appears in the lower sizes is equal to the rate at which it is broken out of larger sizes. If the rate at which dye-containing particles are being selected for breakage is S_0 (s^{-1}), then the rate of change of the mass of tracer (larger than the minimum tracer size) $M_{1-\chi}$ by breakage is

$$\frac{dM_{1-\chi}}{dt} = -S_0(t)M_{1-\chi} \tag{12}$$

It follows that

$$\frac{d}{dt}(1-\chi) = -S_0(t)(1-\chi) \text{ or } \frac{d}{dt}\ln(1-\chi) = -S_0(t) \tag{13}$$

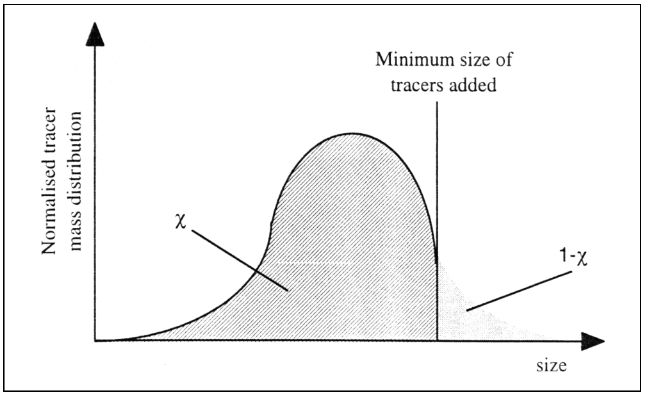

Figure 5. Tracer-mass distribution showing the fraction relegated χ.

Thus, the initial gradient of a plot of ln $(1-\chi)$ against time will have a slope that is related to the instantaneous rate of breakage for size ranges larger than the minimum tracer size. Results obtained this way are correct only in the absence of aggregation back into the original size classes, and in these experiments that is a reasonable constraint only at short times, when the great majority of fragments, and indeed granules, are smaller than the initial tracer spike. However, there is a difficulty in estimating the initial slope, in that the slope at short times varies rapidly. The approach taken here is to use a first-order difference over the first two time points, which in this case will be an underestimate of the selection rate constant. For these two reasons (neglecting of aggregation, underestimation of slope), we can say that the selection rate calculated from Eq. 13 is a lower bound on the actual rate.

Results

In this work, three sizes of tracers granules were used: 180–212 μm, 500–600 μm, and 1,000–1,180 μm. Furthermore, four different ages of tracers were also used: 4 min, 8 min, 12 min, and 16 min. This matrix of conditions allowed the effects of granules age and size on the rate of breakage, to be monitored.

Figure 6 shows a plot of $(1-\chi)$, on a log scale, varying with time for the three different sizes of tracer used: all of these results are from experiments in which 8-min-old tracers were used. The initial slopes are comparable at approximately -0.01 s^{-1}. There is no evidence that the selection rate depends on tracer size. Since we have taken care to show that the tracers behave like the granules, we can assert that the breakage of granules proceeds with constant of approximately 0.01 s^{-1} for granules with an age of 8 min and that the rate constant is independent of granule size.

Figure 7 shows the variation with granule age of the initial breakage rate age (at a constant tracer size of 1,000–1,180 μm). From this plot, it appears that for a 4-min-old tracer there is a much greater breakage rate than at all other times. This implies that there is initially a strong variation in the dependence of the selection rate constant on granule age which then tails off.

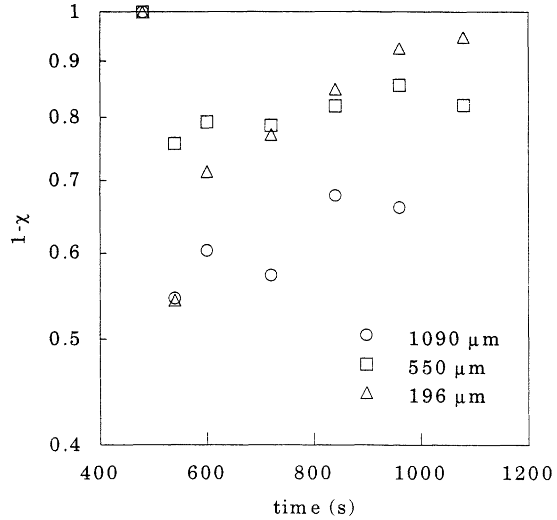

Figure 6. Fraction of tracer relegated for tracers of three different sizes but constant ages of 8 min.

The tracers were all added to a standard experiment at 8 min.

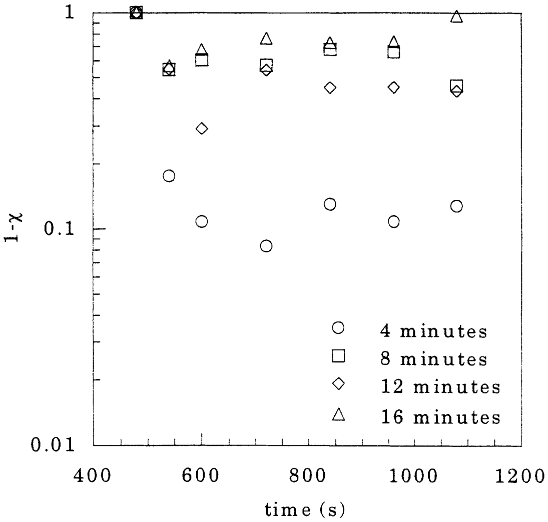

Figure 7. Fraction of tracer relegated for tracers of four different ages but a constant size of 1,090 μm.

The tracers were all added to a standard experiment at 8 min.

Conclusions

In a previous article (Pearson et al., 1998) we showed that there is confounding between the effects of age and size in the kinetics of granulation. In order to increase our understanding of the individual effects of each of these characteristics, tracer granules have been added to some experiments. The first results presented in this article are concerned with verification of the degree to which the tracer granules mimic the standard granules. The results of the experiments carried out have shown that in all three of the areas considered, the behavior of the dye-containing granules is representative of that of the standard granules. Therefore, it has been concluded that these tracer granules mimic the standard granules sufficiently to make their use worthwhile.

At a fundamental level, it has been observed that the dye added to the tracer granule did not remain within the size fraction at which it was added: rather, dyed material appeared in granules both larger than, and smaller than, the initial tracer granules. Therefore, it may be concluded that breakage is definitely occurring as expected. Furthermore, it has been shown that we can make an estimate of the rate at which breakage is occurring, depending both on the size and on the age of the granules. As an initial hypothesis, it is suggested that the rate of breakage depends on the age of the granules, decreasing rapidly initially and then tailing off to a constant rate, but that it is independent of the granule size. These results may be used in determining the kinetics necessary to carry out a satisfactory simulation of the evolution of particle-size distributions with time, as we will show in a future article of this series (Hounslow et al., 2001).

Notation

A_b = spectrophotometric absorption
d = mass of dye, kg
g = mass of granules, kg
h = mass of water, kg
l = particle size, m
M = tracer mass density function, m^{-1}
$M_{1-\chi}$ = mass of dye , not relegated, kg
ΔM = mass of dye on a sieve, kg
p = mass of binder (PEG), kg
s = mass of solid (*Durcal*), kg
t = time, s
x = mass fraction of dye in a solution
w = mass of granules, kg
w = mass density function, $\mathrm{kg}^{-1}\cdot\mathrm{m}^{-1}$

Greek letters

μ = parameter in Eq. 1
ν = parameter in Eq. 1
λ = ratio of liquid/solid in granules
χ = fraction of tracer relegated

Subscript

i = of size class i

Miscellaneous symbol

$\hat{\ }$ = normalized density function

Acronym

PEG = polyethylene glycol

Literature Cited

Hounslow, M. J., J. M. K. Pearson, and T. Instone, "Tracer Studies of High-Shear Granulation: II. Population Balance Modelling," in press, *AIChE J.*, (2001).

Knight, P. C., "An Investigation into the Kinetics of Granulation Using a High Shear Mixer," *Powder Technol.*, **77**, 159 (1993).

Knight, P. C., T. Instone, J. M. K. Pearson, and M. J. Hounslow, "An Investigation Into the Kinetics of Liquid Distribution and Growth in High Shear Mixer Agglomeration," *Powder Technol.*, **97**, 246 (1998).

Pearson, J. M. K., M. J. Hounslow, T. Instone, and P. C. Knight, "Granulation Kinetics: The Confounding of Particle Age and Size," *Proc. Int. Symp. Part. Tech.*, Brighton, U.K. (1998).

Ramaker, J., M. A. Jelgersma, C. Gillaume, P. Vonk, and N. Kossen, "Scale Down of High-Shear Pelletization," *Control of Particulate Processes IV*, Delft, The Netherlands, **39**, 41 (1997).

Scott, A. C., M. J. Hounslow, and T. Instone, "Direct Evidence of Heterogeneity During High-Shear Granulation," *Powder Technol.*, **113**, 205 (2000).

Manuscript received Nov. 23, 1999, and revision received Feb. 12, 2001.